Physics – Uspekhi **40** (11) 1149 – 1160 (1997)

REVIEWS OF TOPICAL PROBLEMS PACS numbers: 41.20.Jb, 42.25.Ja, **78.90.+t**, 84.40.Cb

Chiral electromagnetic objects

B Z Katsenelenbaum, E N Korshunova, A N Sivov, A D Shatrov

Contents

Abstract. A review is presented of some recent theoretical results in the research and development work on artificial spatially dispersive media and on structures possessing chiral properties in the microwave range. The results discussed are mainly obtained for chiral objects taken in the form of long helices of small radius to wavelength ratio, and of arrays of such helices. These structures display strong polarization-selective resonance effects which give rise to a rich variety of their electrodynamic properties.

1. Introduction. A phenomenological theory

This paper is a review of some recent theoretical results obtained in a new trend of the theory and the application of artificial media with spatial dispersion, known as chiral media. This trend deals with media which exhibit chiral properties in the radiowave range at the centimetre and millimetre scales rather than in the optical range (optical activity). The chiral effects are related to symmetrical properties of elements, which are used to produce the artificial medium. The potentialities of the artificial media are wider than in the optical range, where chirality is determined by the properties of molecules, since their constituents can possess a complicated structure. In particular, they may show resonant characteristics, though their size is small compared to the wavelength.

Artificial chiral media can be not only 'three-dimensional' but also thin with regard to the wavelength. The new results discussed in the paper were mainly obtained for chiral objects such as long helices of small radius, arrays of such helices and cascades of these arrays. These objects were found to posses a wide variety of electrodynamic properties.

At present a lot of research groups from Finland, the USA, Belorussia, Russia, France, Germany and South Africa are involved in theoretical and experimental studies of artificial chiral media. International conferences on these objects have been held since 1993. The latest one took place in Russia in 1996. The references of the conference proceedings [1] list 109 works devoted to the electrodynamics of artificial media, carried out during 1995 only. The problem is considered comprehensively in Ref. [2].

The Introduction outlines the foundations of a phenomenological theory and some basic results, in particular, new data obtained in the framework of the theory (Sections 1.3 and 1.4).

1.1 Spatial dispersion. Constitutive relations

The idea that there is a one-to-one correspondence between the electric induction $\mathbf{D}(\mathbf{r}, t)$ and electric field strength $\mathbf{E}(\mathbf{r}, t)$ (we use hereafter the Gaussian CGS system of units)

$$\mathbf{D}(\mathbf{r}, t) = \varepsilon \mathbf{E}(\mathbf{r}, t)\,, \tag{1.1}$$

where the permittivity ε (scalar or tensor) depends on the properties of the medium, requires, as is known, two refinements. In the general case statement (1.1) that the electric displacement $\mathbf{D}(\mathbf{r}, t)$ depends only on $\mathbf{E}(\mathbf{r}, t)$ determined at the same point and moment is not correct.

One refinement consists in the fact that the electric displacement $\mathbf{D}(\mathbf{r}, t)$ depends not only on $\mathbf{E}(\mathbf{r}, t)$ but also on its time derivative. For an arbitrary dependence of $\mathbf{E}(\mathbf{r}, t)$ on t, Eqn (1.1) is not valid. However, when the field follows the harmonic dependence, i.e. there are time-independent vectors

B Z Katsenelenbaum Institute of Radio Engineering and Electronics, Russian Academy of Sciences,
ul. Mokhovaya 11, 103907 Moscow, Russia
Tel. (7-095) 203 48 36
Fax (7-095) 203 84 14
E N Korshunova, A N Sivov, A D Shatrov Institute of Radio Engineering and Electronics, Russian Academy of Sciences,
pl. Vvedenskogo 1, 141120 Fryazino, Moscow Region, Russia
Tel. (7-095) 526 92 66
Fax (7-095) 203 84 14

Received 29 May 1997
Uspekhi Fizicheskikh Nauk **167** (11) 1201 – 1212 (1997)
Translated by G N Chuev; edited by A Radzig

$\mathbf{E}(\mathbf{r})$ and $\mathbf{D}(\mathbf{r})$ (which are complex amplitudes):

$$\mathbf{E}(\mathbf{r},t) = \mathrm{Re}\left[\mathbf{E}(\mathbf{r})\exp(\mathrm{i}\omega t)\right],$$
$$\mathbf{D}(\mathbf{r},t) = \mathrm{Re}\left[\mathbf{D}(\mathbf{r})\exp(\mathrm{i}\omega t)\right], \qquad (1.2)$$

then Eqn (1.1) is correct, but the coefficient ε depends on the frequency, $\varepsilon = \varepsilon(\omega)$. This frequency dependence may not be taken into account only when the Fourier (temporal) spectrum of these quantities is 'rather narrow', i.e. the process is close to the harmonic one. Further we will consider only the harmonic processes and refer to $\mathbf{E}(\mathbf{r})$ and $\mathbf{D}(\mathbf{r})$ as the electric field strength and displacement, respectively. The complex amplitudes $\mathbf{H}(\mathbf{r})$ and $\mathbf{B}(\mathbf{r})$, i.e. the magnetic field strength and induction, are introduced in a similar manner.

The other refinement deals with spatial dispersion, i.e. with the fact that the electric displacement $\mathbf{D}(\mathbf{r})$ depends not only on $\mathbf{E}(\mathbf{r})$ but also on its spatial derivatives. In the media where this effect is substantial, formula (1.1) is not correct for arbitrary spatial dependences of the fields. Only when the fields vary in space as in a plane wave (at least locally), this formula still holds, but ε depends on the direction of the normal $\mathbf{N}$ to the wave front:

$$\mathbf{D}(\mathbf{r}) = \varepsilon(\mathbf{N})\mathbf{E}(\mathbf{r}). \qquad (1.3)$$

The permittivity $\varepsilon(\mathbf{N})$ is a tensor and not a scalar even in an isotropic medium.

For arbitrary dependences of the fields on $\mathbf{r}$, the first spatial derivatives of $\mathbf{E}(\mathbf{r})$ enter the electric displacement $\mathbf{D}(\mathbf{r})$ only through the combination $\mathrm{rot}\,\mathbf{E}(\mathbf{r})$ [3]. Since the fields $\mathbf{D}(\mathbf{r})$ and $\mathbf{E}(\mathbf{r})$, as well as $\mathbf{B}(\mathbf{r})$ and $\mathbf{H}(\mathbf{r})$ for harmonic oscillations in points with no extraneous currents satisfy the homogeneous Maxwell equations

$$\mathrm{rot}\,\mathbf{H} = \mathrm{i}k\mathbf{D}, \qquad \mathrm{rot}\,\mathbf{E} = -\mathrm{i}k\mathbf{B} \qquad \left(k = \frac{\omega}{c}\right), \qquad (1.4)$$

the constitutive relations linking these vectors can be written in the symmetric form excluding their explicit derivatives:

$$\mathbf{D} = \varepsilon\mathbf{E} - \mathrm{i}\varkappa\mathbf{H}, \qquad \mathbf{B} = \mu\mathbf{H} + \mathrm{i}\varkappa\mathbf{E}. \qquad (1.5)$$

Here ε, μ, and $\varkappa$ are the material constants, which do not depend on the field structure [cf. (1.3)]. There are some other forms of these relations in the literature, which are equivalent in essence.

The cross-terms arising in (1.5) can be explained without considering the nonlocal dependence of $\mathbf{D}$ on $\mathbf{E}$ (and correspondingly $\mathbf{B}$ on $\mathbf{H}$). The term proportional to $\mathbf{H}$, which is included in $\mathbf{D}$, means that a current induced by an alternating magnetic field in the elements of a chiral medium causes not only a magnetic dipole moment but also an electric dipole moment. Due to the reciprocity requirement, the alternating electric field induces in such elements the current which in turn gives rise to both the electric and magnetic dipole moments, i.e. the magnetic flux density is also proportional to $\mathbf{E}$.

In media with no absorption effects the material constants ε, μ, and $\varkappa$ are real. Notice that the coefficients of the cross-terms in (1.5) are complex conjugated, since the medium properties should be otherwise nonreciprocal.

We assume the constants ε, μ, and $\varkappa$ to be scalar, i.e. we consider isotropic chiral media, which are most interesting for radiophysics.

In the next three sections we consider some formal properties of solutions to the homogeneous Maxwell equations satisfying constitutive relations (1.5).

1.2 Generalized circular polarization

The electrodynamic behaviour of any homogeneous medium can be naturally characterized by the field structure pertinent to eigenwaves, which can propagate in the medium along an axis z so that all the components of the waves depend on z via the factor $\exp(-\mathrm{i}hz)$. In an isotropic unbound medium the axis z can be any straight line.

In an achiral medium ($\varkappa = 0$) the eigenwaves are, for example, two linearly polarized plane waves:

$$E_x = \exp(-\mathrm{i}hz), \qquad H_y = \frac{1}{\eta}\exp(-\mathrm{i}hz), \qquad (1.6a)$$

$$E_y = \exp(-\mathrm{i}hz), \qquad H_x = -\frac{1}{\eta}\exp(-\mathrm{i}hz), \qquad (1.6b)$$

where

$$h = kn, \qquad n = \sqrt{\varepsilon\mu}, \qquad \eta = \sqrt{\frac{\mu}{\varepsilon}}. \qquad (1.7)$$

These waves have the same propagation constants h and any linear combination of the waves is the eigenwave too. If the coefficients of this linear combination are complex, then the wave need not be linearly polarized.

In a chiral medium ($\varkappa \neq 0$), the waves corresponding to (1.6) cannot exist independently, only two of their linear combinations are eigenwaves

$$E_x = \exp(-\mathrm{i}h_+z), \qquad E_y = -\mathrm{i}\exp(-\mathrm{i}h_+z),$$
$$H_x = \frac{\mathrm{i}}{\eta}\exp(-\mathrm{i}h_+z), \qquad H_y = \frac{1}{\eta}\exp(-\mathrm{i}h_+z), \qquad (1.8a)$$
$$E_x = \exp(-\mathrm{i}h_-z), \qquad E_y = \mathrm{i}\exp(-\mathrm{i}h_-z),$$
$$H_x = -\frac{\mathrm{i}}{\eta}\exp(-\mathrm{i}h_-z), \qquad H_y = \frac{1}{\eta}\exp(-\mathrm{i}h_-z). \qquad (1.8b)$$

The propagation constants of these waves are different and

$$h_\pm = k(n \pm \varkappa), \qquad (1.9)$$

the wave corresponding to (1.8a) is left-hand circularly polarized, while the other wave (1.8b) has right-hand circular polarization.

In these waves the electric and magnetic fields are coupled by the relations

$$\mathbf{H}_\pm = \pm\frac{\mathrm{i}}{\eta}\mathbf{E}_\pm. \qquad (1.10)$$

In a chiral medium any fields $\mathbf{E}_+$, $\mathbf{H}_+$, and $\mathbf{E}_-$, $\mathbf{H}_-$ satisfying relations (1.10) can exist independently. These fields are naturally referred to as the fields with generalized circular polarization [4] (see, also Ref. [5]). The upper sign in (1.10) corresponds to the left-hand circular polarization, the lower sign to the right-hand one.

Any field $\mathbf{E}$, $\mathbf{H}$ can be written as the sum of two fields with generalized circular polarization:

$$\mathbf{E} = \mathbf{E}_+ + \mathbf{E}_-, \qquad \mathbf{H} = \mathbf{H}_+ + \mathbf{H}_-, \qquad (1.11)$$

where

$$\mathbf{E}_\pm = \frac{1}{2}(\mathbf{E} \mp \mathrm{i}\eta\mathbf{H}), \qquad \mathbf{H}_\pm = \frac{1}{2}\left(\mathbf{H} \pm \frac{\mathrm{i}}{\eta}\mathbf{E}\right). \tag{1.12}$$

Substituting (1.10) into (1.5), we arrive at

$$\mathbf{D}_\pm = \varepsilon_\pm \mathbf{E}_\pm, \qquad \mathbf{B}_\pm = \mu_\pm \mathbf{H}_\pm, \tag{1.13}$$

where

$$\varepsilon_\pm = \varepsilon\left(1 \pm \frac{\varkappa}{n}\right), \qquad \mu_\pm = \mu\left(1 \pm \frac{\varkappa}{n}\right). \tag{1.14}$$

Thus, in a chiral medium for fields with generalized circular polarization the Maxwell equations and constitutive relations have the same form as in an achiral medium, but the equivalent material parameters differ for the fields with different circular polarizations (see, for example, Ref. [6]).

Notice that according to (1.10) the Maxwell equations are reduced to the single first-order equation

$$\mathrm{rot}\,\mathbf{E}_\pm = \pm k n_\pm \mathbf{E}_\pm, \tag{1.15}$$

where

$$n_\pm = n \pm \varkappa. \tag{1.16}$$

The first equation in (1.13) has the same meaning as relation (1.3), but it applies not to locally plane waves but to the fields following (1.10), and the quantities $\varepsilon_\pm$ for these fields depend only on the point considered, in contrast to $\varepsilon(\mathbf{N})$.

1.3 Chirality as a perturbation removing degeneracy. Waveguides filled with a chiral medium

Filling a waveguide with a chiral medium reveals some new properties of eigenwaves (see Refs [1, p. 227], [7]). Here we consider only one of the most essential such properties, namely, the chiral effect in the case when the system of waves in the guide at $\varkappa = 0$ is degenerate.

According to (1.8) and (1.9), in an unbound medium the chiral effect removes the degeneracy of plane waves with different directions of linear polarizations. This well-known result could also be found by perturbation theory, supposing the coefficient $\varkappa$ to be a small perturbation parameter. It makes no sense to use this approximate method for the above problem, since the latter has a simple exact solution. However, accurate methods for the problem considered below require cumbersome numerical procedures and they differ for waveguides with different cross-sections, while calculations by the approximate method assume an elementary character and can be applied to a wide class of waveguides. We present here only the statement of the problem and the final result [8].

We consider a circular or square dielectric waveguide or closed waveguides with the same cross-section, which are filled with dielectric material (perhaps not completely). In such waveguides and in many other waveguides of more complicated cross-sections filled with an achiral substance there occur two waves with mutually perpendicular polarizations and equal propagation constants. In this case, the change from an achiral filling substance to a chiral one results in a drastic effect, i.e. removal of the degeneracy. The eigenwaves in the chiral waveguide acquire different propagation constants and well-defined polarizations.

We write the propagation constants of the eigenwaves in an unbound chiral medium (1.9) as

$$h = h_0 \pm \Delta h, \tag{1.17}$$

where $h_0 = kn$ is the propagation constant in the achiral medium, $\Delta h = k\varkappa$.

The perturbation theory yields the following result. The propagation constants in the waveguides also occur symmetrically split and the relations for the constants pertinent to both the propagating waves are the same as (1.17), where h_0 is the propagation constant of degenerate waves in the achiral waveguide, while Δh is determined by the formula

$$\Delta h = \alpha k \varkappa, \tag{1.18}$$

where the coefficient α is expressed through the unperturbed fields:

$$\alpha = \int \left(\mathbf{H}^{(1)}, \mathbf{E}^{(2)}\right) \mathrm{d}S. \tag{1.19}$$

Here $\mathbf{H}^{(1)}$ and $\mathbf{E}^{(2)}$ are the fields of both degenerate waves in the achiral waveguide, which have mutually perpendicular polarizations; these fields are normalized so that the power transferred by them is equal to unity. In (1.19) we should integrate the scalar product over the cross-section filled with a dielectric substance. In the zero approximation with respect to the small parameter $\varkappa$, the fields of the eigenwaves have a structure similar to that of plane waves with circular polarization in an unbound medium (1.8).

For a circular closed waveguide and H_{n1}-waves we have $\alpha = 2n/(v^2 - n^2)$, where $J_n'(v) = 0$. For a square waveguide and H_{n0}-waves the degeneracy is eliminated only at odd n and $\alpha = 8/(\pi n)^2$. For example, the coefficient α is equal to 0.84 for the H_{11}-wave and to 0.81 for the H_{10}-wave. In a waveguide filled with a chiral substance the rotation of the polarization plane is approximately 0.2 less than in an unbound medium.

The influence of a small probe on the resonator frequency and the phase velocity in a waveguide was considered in Refs [9, 10]. According to these papers, if degenerate oscillations or waves existed in a rectangular resonator or a cylindrical waveguide before the insertion of a probe, then measuring the change in the resonance frequency or phase velocity, respectively, we can determine the parameter $\varkappa$.

In the case of an open dielectric waveguide, one of the magnitudes of the h constant in (1.17) may be less than the wave number in the external medium. Then the corresponding wave will be leaky, while the waveguide will operate in a unique mode.

1.4 Bodies with an electric and magnetic surface conductance along one direction. The invariance of circular polarization

A circularly polarized wave scattered by the interface between two chiral media generally produces waves with both circular polarizations. It is known that a wave with left-hand circular polarization normally incident on a plane metallic mirror, reflects from the mirror as a right-hand circularly polarized wave. For an ideally reflective plane interface we will find the condition at which such transformation is not the case. Let the left-hand circularly polarized wave (1.8a) be incident on the plane boundary $z = 0$. Then, in the reflected wave the component E_x at the boundary should be equal to $\exp(\mathrm{i}\alpha)$, while the component E_y should differ from E_y for the incident

wave not only by a phase multiply but a sign as well. Hence, the total field at the boundary is equal to $E_x = 1 + \exp(\mathrm{i}\alpha)$, $E_y = -\mathrm{i}\big(1 - \exp(\mathrm{i}\alpha)\big)$. The ratio of these components is a real value, and therefore the total field at the boundary is linearly polarized and has angle $\alpha/2$ with respect to the x axis. Hence, the component of the electric field perpendicular to this direction of the total field is equal to zero. According to (1.10) the component $\mathbf{H}$ should also be zero in the total field direction. Thus, to avoid depolarization at the boundary, a direction t should exist at which

$$E_t = H_t = 0\,. \tag{1.20}$$

This result is easily extended to the case of waves with generalized circular polarization (1.10), scattered by obstacles of arbitrary shape.

The boundary conditions (1.20) describe, for example, a thickly corrugated metal sheet whose grooves are filled with a substance with high permittivity and are a quarter of a wavelength in 'electric' depth. Note that the boundary conditions (1.20) taken at an obstacle surface of an arbitrary shape are sufficient to prove the theorem of the uniqueness of the solution to the Maxwell equations. It is assumed in the proof that the normal component of vector $[\mathbf{E}, \mathbf{H}^*]$ is zero, which means that a power flux through the surface is absent. This also takes place under the boundary conditions (1.20).

Let us prove that these boundary conditions result in the conservation of any one of the generalized circular polarizations (1.10) on scattering by an obstacle of arbitrary shape in the chiral medium.

Let the obstacle be restricted by the surface S, where the boundary conditions (1.20) apply, meaning the local electric and magnetic conductances are ideal in some tangential direction t. The obstacle is held in a field with left-hand circular polarization $\mathbf{E}^0_+$, $\mathbf{H}^0_+$. We denote the scattered field as $\mathbf{E}^{\mathrm{s}}$, $\mathbf{H}^{\mathrm{s}}$. In the far region, the scattered field is a divergent spherical wave. For example, the electric field is written as $\mathbf{E}^{\mathrm{s}} \simeq \mathbf{F}(\varphi, \theta)\exp(-\mathrm{i}kR)/R$, where $\mathbf{F}(\varphi, \theta) = \big\{F_\varphi(\varphi, \theta), F_\theta(\varphi, \theta)\big\}$ is the scattering vector diagram. The boundary conditions (1.20) are written as

$$\big(\mathbf{E}^0_+ + \mathbf{E}^{\mathrm{s}}\big)_t = \big(\mathbf{H}^0_+ + \mathbf{H}^{\mathrm{s}}\big)_t = 0\Big|_S\,. \tag{1.21}$$

Using (1.12), we extract the right-hand circularly polarized component of the scattered field

$$\mathbf{E}^{\mathrm{s}}_- = \frac{1}{2}\big(\mathbf{E}^{\mathrm{s}} + \mathrm{i}\eta\mathbf{H}^{\mathrm{s}}\big)\,. \tag{1.22}$$

Relation (1.21) results in

$$\big(\mathbf{E}^{\mathrm{s}}_-\big)_t = 0\Big|_S\,. \tag{1.23}$$

Using relation (1.15) corresponding to the lower sign, we can easily find for any point:

$$\mathrm{div}\big[\mathbf{E}^{\mathrm{s}}_-, \mathbf{E}^{\mathrm{s}^*}_-\big] \equiv 0\,. \tag{1.24}$$

Integrating (1.24) over the volume restricted by an infinitely far surface S_∞ and by the obstacle surface S, we have

$$\int_{S_\infty}\big[\mathbf{E}^{\mathrm{s}}_-, \mathbf{E}^{\mathrm{s}^*}_-\big]_R\,\mathrm{d}s + \int_S\big[\mathbf{E}^{\mathrm{s}}_-, \mathbf{E}^{\mathrm{s}^*}_-\big]_N\,\mathrm{d}s = 0\,. \tag{1.25}$$

The second term in (1.25) is zero, according to (1.23). As a result, the first term is also zero. The components of the scattering vector diagram for fields with right-hand circular polarization are coupled by $F^-_\theta(\varphi, \theta) = -\mathrm{i}F^-_\varphi(\varphi, \theta)$, therefore the nullifying first term in (1.25) leads to $F^-_\theta = F^-_\varphi = 0$. As is known, this means that $\mathbf{E}^{\mathrm{s}}_-$ is identically zero, and hence $\mathbf{E}^{\mathrm{s}} \equiv \mathbf{E}^{\mathrm{s}}_+$, i.e. the scattering does not change the polarization of the incident field. The case when $\mathbf{E}^0 = \mathbf{E}^0_-$ can be considered similarly.

Clearly, the separation of any field, according to (1.11), takes place in an achiral medium too. This separation remains even if the achiral medium includes scatterers satisfying the boundary conditions (1.20). Thus an artificial chiral medium can be produced by small scatterers frequently and randomly distributed in the achiral medium, which satisfy the boundary conditions (1.20).

The microscopic theory resulting in the constitutive relations (1.5) is fully developed in optics (see, for example, Ref. [11]). But in the radio wave range the problem of determining the material constants ε, μ, $\varkappa$ is formulated differently and implies the calculation of the polarizability for small scatterers of a complicated shape, i.e. the solution of the diffraction problem. The latter is solved only for several chiral elements such as small metal helices [12], open rings with salient ends [13], and spheres with helical electric conductivity [14]. The Möbius strip is also reported to be a chiral element [15]; note that in this case the general method for solving diffraction problems at unoriented surfaces may be appropriate [16].

The calculation of constituent constants in (1.5) for three-dimensional media as well as the general statement of the problem could be a subject of a separate paper and are not considered here. In the next two sections we solve the diffraction problems for the chiral elements such as thin elongated helices and arrays of these helices.

2. Thin cylinders with helical surface conductance as chiral elements

We describe here the physical properties of electromagnetic fields arising due to the diffraction of plane waves at thin elongated anisotropic cylinders with helical conductivity. Such cylinders show resonant properties closely related to the guided waves.

We consider cylinders having combined electric and magnetic helical conductivity or only electric conductivity of the same type.

The latter model well describes (one- or multiturn) coils when the distance between axes of neighbouring wire loops is far less than the wavelength, while the gaps fall in the certain range. The wire is assumed to be thin compared to the helix radius. The good approximation of real coils by the model is experimentally confirmed in Ref. [18], and, in particular, by results from the theoretical consideration made in Ref. [17]. Notice that under certain conditions such objects do not change the direction of circular polarization of incident waves scattered by the objects.

The model of a scatterer in the form of a cylinder with helical electric and magnetic conductivity has ideal chiral properties, i.e. the circular polarization of the incident field remains the same at all conditions in accordance with the results of Section 1.4. As this takes place, the scattered fields differ significantly for waves with different directions of circular polarization. Notice that the model with combined electric and magnetic conductivity is simpler for the mathematical treatment.

2.1 Properties of guided waves

2.1.1 Waves scattered by a cylinder with combined helical conductivity. Let a cylindrical surface of radius a (Fig. 1) satisfy the boundary conditions (1.20) corresponding to ideal electric and magnetic conductivity along the circular helix:

$$E_z \cos\psi + E_\varphi \sin\psi = 0\,, \qquad H_z \cos\psi + H_\varphi \sin\psi = 0\,, \quad (2.1)$$

where ψ is the twist angle. For definiteness, we consider right-hand circular helixes ($0 \leqslant \psi \leqslant \pi/2$). The conditions (2.1) are one-sided, therefore the inner and outer cylindrical regions can be treated independently.

We consider the waves propagating outside the cylinder ($r > a$) and depending on the coordinates φ and z as $\exp(-im\varphi - ihz)$, where h is the longitudinal wavenumber. Not restricting ourselves, we suppose the azimuthal index to be positive ($m \geqslant 0$) as the simultaneous change in sign of m and h corresponds to the same wave propagated in a coordinate system with the opposite direction of the z-axis.

Under the boundary conditions (2.1) the homogeneous Maxwell equations have two types of independent solutions corresponding to circularly polarized waves (in accordance with (1.10) at $\varepsilon = \mu = 1$)

$$\mathbf{H} = \mp i\mathbf{E}\,. \quad (2.2)$$

The upper sign in (2.2) and further denotes right-hand circular polarization, while the lower sign implies left-hand circular polarization. The dispersion equations for transverse wavenumber $g = g' + ig'' = \sqrt{k^2 - h^2}$ used for symmetrical ($m = 0$) and asymmetrical ($m \geqslant 1$) waves take the form [19]

$$\frac{gaH_0^{(2)}(ga)}{H_1^{(2)}(ga)} = \pm vka\,, \quad (2.3)$$

$$h = \pm k - \frac{mv/a}{1 \pm vka\left[H_{m-1}^{(2)}(ga)/gaH_m^{(2)}(ga)\right]}\,, \quad (2.4)$$

where $v = \tan\psi$.

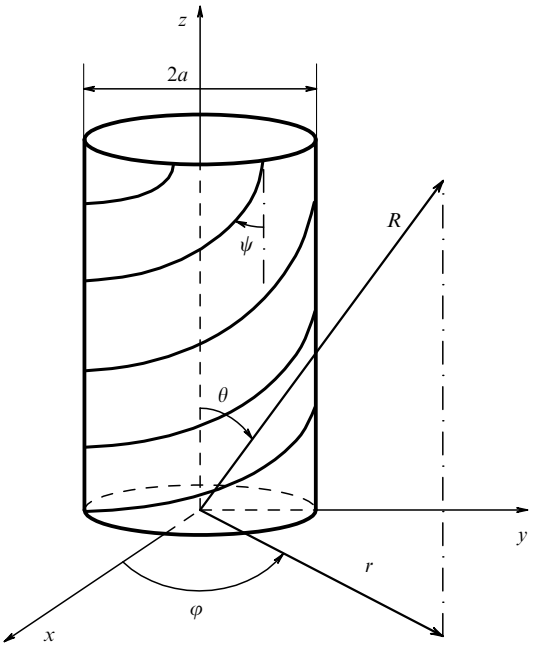

Figure 1. Cylinder with surface helical conductance.

For left-hand circular polarization equation (2.3) has a solution at any twist angle, corresponding to a slow wave ($g' = 0$, $g'' < 0$). The symmetrical wave with the right-hand circular polarization is leaky ($g'' > 0$). For a cylinder of small radius ($ka \ll 1$) the radiative losses of the wave are small ($g'' \ll g'$, $0 < g' < k$).

If the twist angle is zero (and $v = 0$) the asymmetrical waves are TEM-modes ($E_z = H_z = 0$, $h = \pm k$). In this case the electric field is written as

$$E_\varphi = \left(\frac{a}{r}\right)^{m+1} \exp(-im\varphi \mp ikz)\,,$$
$$E_r = \mp iE_\varphi\,, \qquad m \geqslant 1\,. \quad (2.5)$$

It follows that the right-hand wave at $m \geqslant 1$ propagates only along the positive direction of the z axis, while the left-hand wave propagates in the opposite direction. At small angles of twist ($v \ll 1$), the terms in (2.4) which are of the highest order with respect to v yield the expression for the longitudinal wavenumber

$$h = \pm k - m\frac{v}{a}\,. \quad (2.6)$$

As is seen from (2.6), the right-hand circularly polarized waves are fast ($|h| < k$), while the left-hand waves are slow ($|h| > k$). Formula (2.6) for the fast waves only yields the approximate value of the real part of $h = h' + ih''$. To calculate h'', we should take into account higher-order terms in v in (2.4). At small ka, using the perturbation theory, by (2.4) we can find an explicit expression for the radiative losses of a leaky wave. For instance, at $m = 1$ we have

$$h' = k - \frac{v}{a}\,, \qquad h'' = -\frac{\pi k v^2}{2}\,. \quad (2.7)$$

A significant peculiarity of the waveguide at hand is the existence of forward and backward waves, i.e. the waves whose phase and group velocities are the same or opposite in sign, respectively. Varying the waveguide parameters, we can transform waves of a certain type into ones of the other type. According to (2.7), for a wave with azimuthal index $m = 1$ this transition occurs at $ka = v$.

2.1.2 Waves of a hollow cylinder with electric surface helical conductivity [20]. We describe here properties of waves scattered by an anisotropic cylinder whose surface satisfies the Vladimirskiĭ two-side boundary conditions

$$E_z^+ = E_z^-\,, \qquad E_\varphi^+ = E_\varphi^-\,, \qquad E_z \cos\psi + E_\varphi \sin\psi = 0\,,$$
$$\left(H_z^+ - H_z^-\right)\cos\psi + \left(H_\varphi^+ - H_\varphi^-\right)\sin\psi = 0\,. \quad (2.8)$$

The superscripts '+' and '−' correspond to the different sides of the cylindrical surface. The dispersion equation for a wave at the cylinder can be written as

$$\left(h + k + m\frac{v}{a}\right)\left(h - k + m\frac{v}{a}\right) = v^2k^2\,\frac{J_{m-1}(ga)H_{m-1}^{(2)}(ga) + J_{m+1}(ga)H_{m+1}^{(2)}(ga)}{2J_m(ga)H_m^{(2)}(ga)}\,. \quad (2.9)$$

The relevant slow waves are carefully investigated in Ref. [21]. We discuss the properties of leaky and slow waves under the

conditions

$$v \ll 1\,, \qquad ka \ll 1\,. \tag{2.10}$$

These properties are rather close to those considered in Section 2.1.1.

In contrast to (2.3), dispersion equation (2.9) does not have a solution corresponding to a weakly leaking wave at $m = 0$. For asymmetrical waves ($m \geqslant 1$) under conditions (2.10) the right-hand side of (2.9) is small and formula (2.6) is valid for the longitudinal wavenumber.

At $v = 0$, the asymmetrical waves are TEM-modes whose fields outside the cylinder are described by the same formulae (2.5), while inside the cylinder the fields are given by

$$E_\varphi = \left(\frac{r}{a}\right)^{m-1} \exp(-\mathrm{i}m\varphi \mp \mathrm{i}kz)\,, \qquad E_r = \pm\mathrm{i}E_\varphi\,. \tag{2.11}$$

Notice that according to (2.5) and (2.11) the direction of polarization rotation differ inside and outside the cylinder for each wave. Inside the cylinder the fundamental mode ($m = 1$) is a plane wave.

If $v \neq 0$, then under conditions (2.10) the waves retain circular polarization with good accuracy.

Using the perturbation method, the formulae for the real and complex parts of the propagation constant can be derived from (2.9). They differ from (2.7) only in that the damping is twice as small in the case of a hollow cylinder, since the longitudinal flux of power is twice as large due to the presence of the inner cylindrical region.

2.1.3 Waves scattered by a cylinder with electric conducting surface, which is filled with a magnetodielectric substance [22]. We consider the properties of waves guided by a cylinder under the conditions $ka\sqrt{\varepsilon\mu} \ll 1$ and $v \ll 1$, where ε and μ are the permittivity and permeability of the cylinder, respectively. Without writing the cumbersome dispersion equation [22] resulting from the boundary conditions (2.8), we present here only its solution

$$h = \pm k\sqrt{\frac{\mu(\varepsilon+1)}{\mu+1}} - m\,\frac{v}{a} \qquad (m \geqslant 1)\,. \tag{2.12}$$

Notice that taking into account only the terms which have the highest order with respect to ka, the lowest modes ($m = 1$) inside the cylinder are homogeneous plane circularly polarized waves:

$$E_\varphi = \exp(-\mathrm{i}\varphi - \mathrm{i}hz)\,, \qquad H_\varphi = \pm\frac{\mathrm{i}}{\eta}\,E_\varphi\,,$$

$$E_r = \mathrm{i}E_\varphi\,, \qquad H_r = \pm\frac{\mathrm{i}}{\eta}\,E_r\,, \tag{2.13}$$

where the quantity η, which plays the role of the wave resistance, is equal to

$$\eta = \sqrt{\frac{\mu(\mu+1)}{\varepsilon+1}}\,. \tag{2.14}$$

The upper and lower sings in (2.12) and (2.13) are respective. In doing so, the lower signs always correspond to the slow wave, the upper signs to the leaky wave when the value of v/ka, characterizing twisting, lies within the interval

$$\sqrt{\frac{\mu(\varepsilon+1)}{\mu+1}} - 1 < \frac{v}{ka} < \sqrt{\frac{\mu(\varepsilon+1)}{\mu+1}} + 1\,. \tag{2.15}$$

External radiation fields are elliptically polarized in contrast to the internal fields. The coefficient of ellipticity varies from -1 to $+1$ when v/ka lies in the range (2.15). At the twist equal to

$$\frac{v}{ka} = \frac{\varepsilon\mu - 1}{\sqrt{\mu(\varepsilon+1)(\mu+1)}}\,, \tag{2.16}$$

the radiation field is linearly polarized and is emitted at an angle θ with respect to the z-axis, which is given by

$$\theta = \arccos\sqrt{\frac{\mu+1}{\mu(\varepsilon+1)}}\,. \tag{2.17}$$

The main property of the two lowest modes ($m = 1$) is that they are homogeneous circularly polarized plane waves with opposite directions of rotation and different propagation constants inside the cylinder. Such property is known to be exhibited by waves in homogeneous unbound chiral media, described by constitutive relations (1.5). The equivalent constituent parameters $\tilde{\varepsilon}$, $\tilde{\mu}$, and $\tilde{\varkappa}$ (permittivity, permeability, and chiral coefficient) are obtained by comparison of formulae (2.12)–(2.14) with relations (1.7)–(1.9) for the fields in an unbound chiral medium:

$$\tilde{\varepsilon} = \frac{\varepsilon+1}{\mu+1}\,, \qquad \tilde{\mu} = \mu\,, \qquad \tilde{\varkappa} = -\frac{v}{ka}\,. \tag{2.18}$$

Thus, the considered waveguide structures show strong chiral effects, i.e. the guided-by-them waves with circular polarization and opposite signs of polarization rotation are principally different. In contrast to the waveguides filled with a chiral medium (see Section 1.3), this difference results from the helical conductivity of the surface.

2.2 Low-frequency resonances in isolated cylinders under diffraction of plane waves

Resonance effects occur at low frequencies ($ka \ll 1$), when a plane wave is diffracted by isolated cylinders with helical surface conductivity. These effects are manifested, in particular, by a sharp increase in the scattering cross-section and tightly related to the weakly leaking waves described in Section 2.1. The peculiarity of the scatterers is that the resonances arise only for a certain sign of polarization rotation of the incident wave. Below we discuss the resonant effects for cylinders of the three types considered above.

2.2.1 Scattering by a cylinder with combined electric and magnetic helical surface conductivity [23]. The plane circularly polarized wave

$$E_z^0 = \pm\mathrm{i}H_z^0 = \exp(-\mathrm{i}hz - \mathrm{i}gx)\,, \tag{2.19}$$

where $h = k\cos\theta$ and $g = k\sin\theta$, is incident on a cylinder at angle θ with respect to its axis ($0 < \theta < \pi/2$). The scattering problem reduces to calculation of the two-dimensional scalar function $u(r, \varphi)$, which is related to the component E_z by the dependence

$$E_z = u\exp(-\mathrm{i}hz)\,. \tag{2.20}$$

This function u satisfies the Helmholtz equation and can be presented as the sum of two terms corresponding to the incident and scattered fields:

$$u = \exp(-igr\cos\varphi) + u^{s}(r,\varphi)\,,$$

here the asymptotic of u^{s} is determined by the scattering pattern $\Phi(\varphi)$:

$$u^{s} \simeq \Phi(\varphi)\frac{\exp(-igr)}{\sqrt{gr}}\,. \tag{2.21}$$

In the whole region the scattered field is given by

$$u^{s} = \sum_{m=-\infty}^{\infty} A_m H_m^{(2)}(gr)\exp(-im\varphi)\,. \tag{2.22}$$

Taking into account the boundary conditions (2.1) for the combined conductivity, we find explicit expressions for the coefficients A_m. At $ka \ll 1$, these coefficients are small almost without exception, and they increase sharply in resonance only on excitation with the wave of right-hand circular polarization and reach

$$A_m = -(-i)^m\,. \tag{2.23}$$

For the zero harmonic ($m = 0$), the resonance frequency is determined by the equation

$$\left(\ln\frac{\gamma ka\sin\theta}{2}\right)ka\sin^2\theta + v = 0\,, \qquad \gamma = 1.781\,. \tag{2.24}$$

For other harmonics, the explicit expressions for resonance frequencies are written as

$$ka = \frac{mv}{1-\cos\theta}\,, \qquad m > 0\,, \tag{2.25}$$

$$ka = -\frac{mv}{1+\cos\theta}\,, \qquad m < 0\,. \tag{2.26}$$

At frequencies far from the resonance, the scattered field is weak ($|\Phi(\varphi)| \ll 1$). At the resonance frequency, the scattering pattern determined by the dominant term in (2.22) is given by

$$\Phi(\varphi) = -\sqrt{\frac{2}{\pi}}\exp\left(\frac{i\pi}{4} - im\varphi\right)\,. \tag{2.27}$$

Notice that the resonances in the scattering problem are related to leaky waves guided by the cylinder. The expressions for the expansion coefficients A_m have resonant denominators depending on the incident angle θ. Equating these denominators to zero and allowing for complex angles θ, we arrive at the dispersion equations (2.3) and (2.4) for guided waves. In doing so, the resonance frequencies (2.25) correspond to the forward waves, while the frequencies (2.26) correspond to the backward waves. Note also that at certain angles θ the resonances for harmonics with different azimuthal indices coincide. For example, at normal incidence ($\theta = \pi/2$), following (2.25) and (2.26) the resonance occurs at frequencies

$$ka = |m|v \tag{2.28}$$

for the harmonics with different signs of azimuthal index. The scattering pattern is written then as

$$\Phi(\varphi) = -2\sqrt{\frac{2}{\pi}}\exp\frac{i\pi}{4}\cos m\varphi\,. \tag{2.29}$$

But if $\theta = \arccos(1/3)$, the harmonics with $m = 1$ and $m = -2$ are resonant at the frequency

$$ka = \frac{3v}{2}\,. \tag{2.30}$$

The corresponding scattering pattern is determined by

$$\Phi(\varphi) = -2\sqrt{\frac{2}{\pi}}\exp\left(\frac{i\pi}{4} + \frac{i\varphi}{2}\right)\cos\frac{3\varphi}{2}\,. \tag{2.31}$$

In this case there is no backscattering $(\Phi(\pi) = 0)$.

2.2.2 Scattering by a hollow cylinder with electric helical conductivity [24, 25]. The problem of circularly polarized plane waves scattered by a hollow cylinder under the boundary conditions (2.8) is not reduced to the calculation of a scalar function as in Section 2.2.1, since depolarization takes place, i.e. the scattered field includes waves of both circular polarizations. The problem is solved by expanding the longitudinal components of electric and magnetic field strengths E_z and H_z inside and outside the cylinder in cylindrical functions with an azimuthal factor of $\exp(-im\varphi)$. In doing so, the expansion coefficients for the scattered field are found in an explicit form.

Similar features of waves leaking from the cylinder with combined conductivity and the hollow cylinder with electric conductivity lead to analogous resonance effects in the relevant diffraction problems. Figure 2 shows the frequency dependence of the total scattering cross-section σ_s for circularly polarized waves at normal incidence ($\theta = \pi/2$) on a cylinder with twist angle $\psi = 18°$. The solid line has resonances and corresponds to excitation with the wave of right-hand circular polarization. The smooth dashed line corresponds to excitation with the left-hand wave. The positions of peaks are well described by formulae (2.28) for the resonance frequencies of the cylinder with combined conductivity.

Notice that even at $ka \to 0$ [following (2.28) $\psi \to 0$] the finite disturbance of the total scattered power is observed at resonance and $\sigma_s \to 4\lambda/\pi$.

At the main resonance ($m = 1$) the magnetic and electric fields are uniform and parallel inside the cylinder, being perpendicular to the cylinder axis and to the direction of

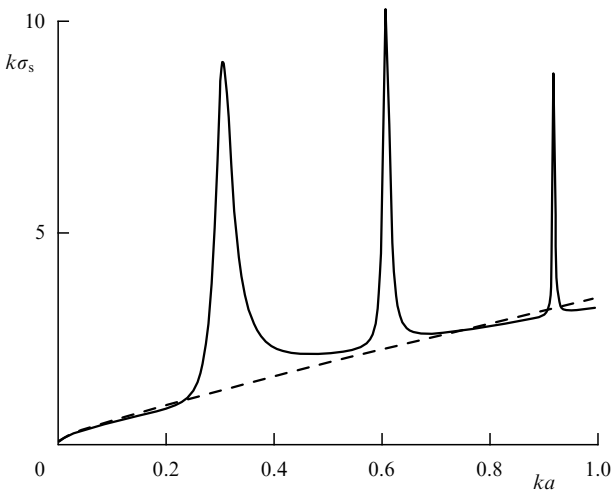

Figure 2. Frequency dependence of the total scattering cross-section.

incident wave propagation. On the excitation with a right-hand circularly polarized plane wave of unit amplitude and accounting only for highest-order terms, these fields are

$$E_y^+ = -\mathrm{i}H_y^+ = \frac{4}{\pi(ka)^2}\,. \tag{2.32}$$

Outside the cylinder in the statical proximity to it, the fields are described by the expressions

$$E_x^- = \mathrm{i}H_x^- = -\frac{4\sin 2\varphi}{\pi(kr)^2}\,, \qquad E_y^- = \mathrm{i}H_y^- = \frac{4\cos 2\varphi}{\pi(kr)^2}\,. \tag{2.33}$$

Following (2.32) and (2.33) under the resonance conditions, the stored reactive power is the same for the inner and outer cylinder regions. Figure 3 plots electric and magnetic force lines pertinent to fields (2.32), (2.33). The fields outside the cylinder can be considered as fields induced by an infinite set of electric and magnetic dipoles located at the z axis and oriented in the y direction. The above-sketched low-frequency resonance differs in principle from the widely-known Helmholtz resonance (see, for example, Ref. [26]) by the unusual field distribution and high quality.

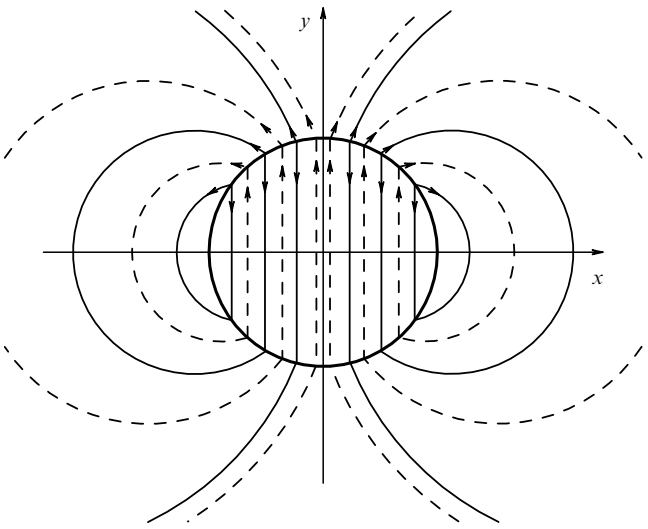

Figure 3. Electric (solid curves) and magnetic (dashed curves) force lines at the low-frequency resonance.

2.2.3 Scattering by a cylinder with electric helical surface conductivity, which is filled with a magnetodielectric substance [27]. Filling the cylinder with a magnetodielectric substance makes the scattered field elliptically polarized even at resonance on exposure to incident circularly polarized waves. Additionally, thermal losses arise in a nonideal dielectric. For example, we consider elliptically polarized unit plane waves, which are normally incident on the cylinder. For materials with low dielectric losses ($\varepsilon = \varepsilon' - \mathrm{i}\varepsilon''$, $\varepsilon'' \ll \varepsilon'$), formula (2.12) leads to the expression for resonance frequencies

$$ka = |m|\sqrt{\frac{\mu+1}{\mu(\varepsilon'+1)}}\,v\,. \tag{2.34}$$

Under conditions $ka\sqrt{\varepsilon'\mu} \ll 1$ and $v \ll 1$, the expression for the quality of the main resonance takes the form

$$Q = \frac{2(\varepsilon'+1)}{\pi v^2(2+\varepsilon'+1/\mu)+2\varepsilon''(\varepsilon'+1)}\,. \tag{2.35}$$

The influence of the polarization of the incident wave on the scattered and absorbed powers is as follows. The scattering and absorption have maxima at the resonance frequency (2.34), when the incident wave is right-hand polarized and the coefficient of ellipticity is

$$K = \sqrt{\frac{\mu+1}{\mu(\varepsilon'+1)}} \qquad \left(\sqrt{\varepsilon'\mu} > 1\right). \tag{2.36}$$

In this case the major axis of polarization ellipse is directed along the z axis. The left-hand wave with the same coefficient of ellipticity and the axes of polarization ellipse turned through 90° does not excite the resonance and therefore weakly interacts with the cylinder.

At the resonance, the scattering patterns for the components E_z and $E_\varphi = H_z$ are proportional to $\cos\varphi$ [sf. (2.29)]; in this case the electric field far from the cylinder has right-hand polarization and the same coefficient of ellipticity (2.36).

The intensity absorbed at resonance is not a monotonic function of ε''. It has a maximum at

$$\varepsilon'' = \frac{\pi(1+2\mu+\varepsilon'\mu)}{2\mu(1+\varepsilon')}\,v^2\,. \tag{2.37}$$

The quality of the resonance decreases twofold for this value of ε'' as compared to the case when there are no dielectric losses. Under the conditions (2.37) and for the above polarization of the incident wave (2.36), the absorption cross-section σ_a is equal to the scattering cross-section σ_s:

$$\sigma_a = \sigma_s = \frac{\lambda}{\pi}\,. \tag{2.38}$$

With no dielectric loss ($\varepsilon'' = 0$), the maximum of scattering cross-section exceeds the above value by a factor of 4 and coincides with that for a hollow cylinder (see Section 2.2.2).

Figures 4 and 5 plot the frequency dependences of the absorption and scattering cross-sections for the cylinder with

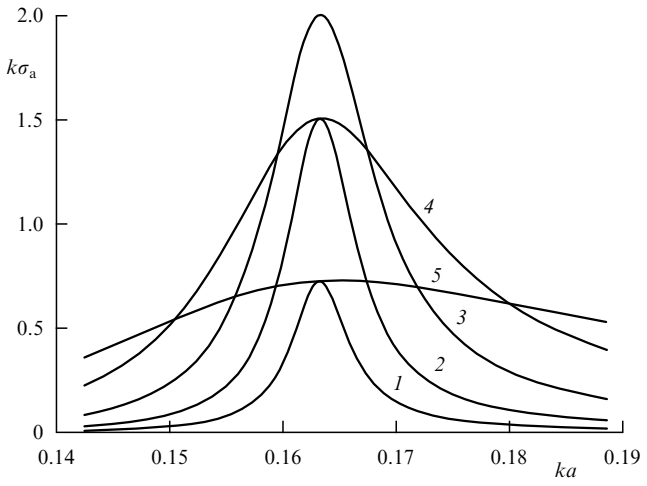

Figure 4. Frequency dependence of the absorption cross-section at $v = 0.2$, $\varepsilon' = 2$, $\mu = 1$ and various ε'': (*1*) $\varepsilon'' = 0.012$, (*2*) $\varepsilon'' = 0.035$, (*3*) $\varepsilon'' = 0.105$, (*4*) $\varepsilon'' = 0.314$, and (*5*) $\varepsilon = 0.942$.

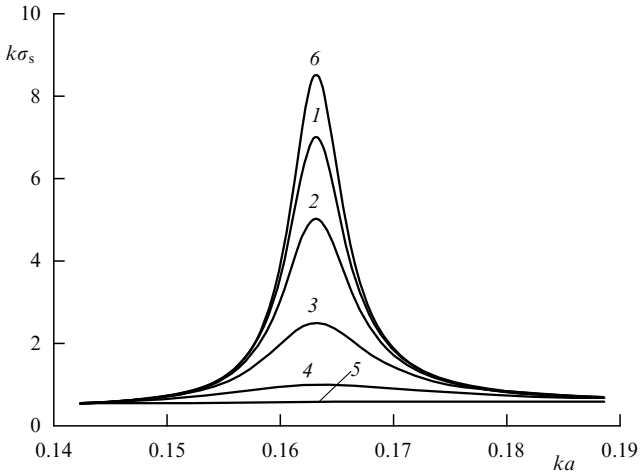

Figure 5. Frequency dependence of the scattering cross-section at $v = 0.2$, $\varepsilon' = 2$, $\mu = 1$ and various ε'': (*1*) $\varepsilon'' = 0.012$, (*2*) $\varepsilon'' = 0.035$, (*3*) $\varepsilon'' = 0.105$, (*4*) $\varepsilon'' = 0.314$, (*5*) $\varepsilon'' = 0.942$, and (*6*) $\varepsilon'' = 0$.

$v = 0.2$, $\varepsilon' = 2$, and $\mu = 1$ at various values of ε''. As is seen from the figures, the scattering cross-section σ_s monotonically depends on ε'' in contrast to σ_a.

3. Diffraction at arrays of cylinders with helical surface conductance

First, we outline the results of studying the plane waves normally incident on isolated arrays formed by cylinders with helical surface conductivity (Fig. 6). We consider arrays of two types: from cylinders with combined surface conductivity [following boundary conditions (2.1)] and from hollow cylinders with electric surface conductivity [boundary conditions (2.8)]. The array period p is assumed to be less than the wavelength λ, ensuring the absence of side lobes. The arrays are characterized by three parameters such as the angle ψ of twisting of the conducting helices, the fill factor $q = 2a/p$ and the normalized period $s = p/\lambda$. The quantities q and s fall within the range $(0, 1)$.

Finally, we describe filtration and chirotropic properties of a cascade from two arrays.

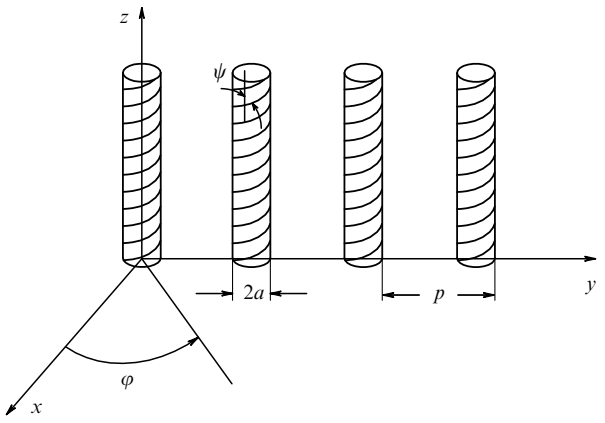

Figure 6. The general view of the array of cylinders with helical surface conductivity.

3.1 Array of cylinders with electric and magnetic surface conductance

The problem of circularly polarized plane waves normally incident on an array of cylinders with combined surface conductivity is reduced to the calculation of a scalar function $u(x, y) = E_z$ satisfying the homogeneous Helmholtz equation

$$\Delta u + k^2 u = 0 \tag{3.1}$$

under boundary conditions of the third kind on the surface of each cylinder

$$v \frac{\partial u}{\partial (kr)} \pm u = 0\,, \tag{3.2}$$

where r is the local radial coordinate. The upper and lower signs correspond to the right-hand and left-hand circular polarizations, respectively. Far from the arrays $(|x| \gg p)$, the function u takes the form

$$\begin{aligned} u &= \exp(-\mathrm{i}kx) + R\exp(\mathrm{i}kx) \qquad (x < 0)\,, \\ u &= T\exp(-\mathrm{i}kx) \qquad\qquad\quad (x > 0)\,, \end{aligned} \tag{3.3}$$

where R and T are the required reflection and transmission coefficients. An infinite set of linear algebraic equations for coefficients of the function u expanded in a Fourier series on the cylindrical surface are found in Ref. [28]. The quantities R and T are expressed by these coefficients via simple formulae.

On excitation with right-hand circularly polarized waves some effects arise in the array, which are related to low-frequency resonances in isolated cylinders. The conditions of the resonances are determined by (2.24) – (2.26) at $\theta = \pi/2$. In the vicinity of the resonances, the coefficients R and T change sharply. Figure 7 depicts the dependence of absolute values of the transmission coefficient on s for the waves with right-hand (solid line) and left-hand (dashed line) circular polarization, scattered by an array with parameters $q = 0.04$ and $\psi = 5°$. At the resonance $m = 0$, the waves are completely reflected, while in the vicinity of the resonance $m = 1$ complete reflection as well as complete transmission take place. The left-hand wave is subjected to an almost complete transmission over the whole range of s, thus, the array is an effective polarized filter, for example, at the zero resonance.

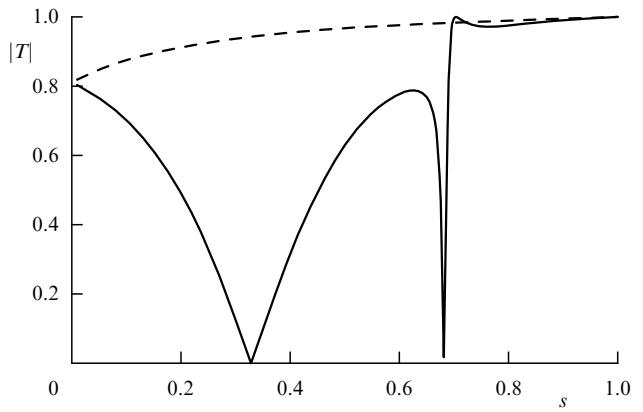

Figure 7. Frequency dependences of absolute values of the transmission coefficient for the right-hand (solid line) and left-hand (dashed line) circularly polarized waves at $q = 0.04$, $\psi = 5°$.

3.2 Array of hollow cylinders with electric surface conductance

In this case the diffraction problem is not reduced to the calculation of a scalar function as in the previous section. Complicated polarization phenomena arise in this situation and the arrays can be used to transform various types of polarization. The method for calculating these arrays is described in detail in Ref. [29]. The matrix reflection and transmission coefficients are expressed by coefficients of the Fourier expansion for the current at the cylindrical surface. These coefficients satisfy an infinite set of linear algebraic equations. We describe below the electrodynamic properties of the arrays revealed.

3.2.1 Semi-transparent shields for circularly polarized waves. Circularly polarized waves exciting an array were studied in Refs [30, 31]. The authors found a relationship between the three array parameters ψ, q, and s at which the transmitted and reflected waves are circularly polarized and retain the same direction of polarization rotation as the incident wave. Figure 8 shows the dependences of q and s on ψ for this class of arrays. The dependences of the amplitudes and phases of transmission coefficients $|t_{r,l}|$ and $\beta_{r,l}$ on the twist angle ψ are shown in Figs 9 and 10 for the right- and left-hand circularly polarized waves. As is seen from Figs 8 and 9, at $\psi = 55°$, $q = 0.87$, and $s = 0.38$ the array completely reflects the left-hand circularly polarized wave and partially transmits the right-hand wave.

3.2.2 Transducers of polarization as power dividers. The array parameters can be chosen so that the incident linearly polarized wave $E_y = \cos\theta \exp(-ikx)$, $E_z = \sin\theta \exp(-ikx)$ is transformed into two circularly polarized waves, the transmitted and reflected waves having opposite directions of polarization rotation. The relationship between the four parameters θ, ψ, q, and s providing such transformation was found in [31]. The transformation can be carried out using two classes of arrays corresponding to the left- and right-hand circular polarizations of the transmitted wave.

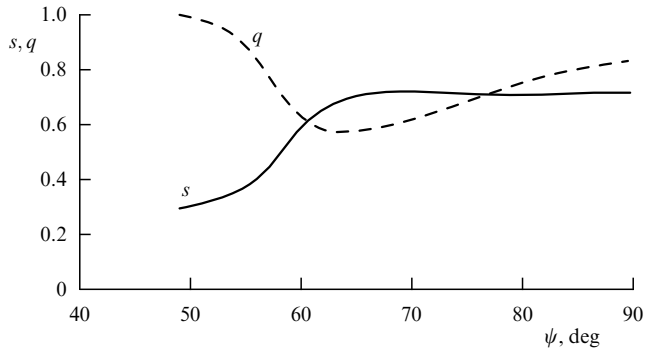

Figure 8. Dependences of q and s on the twist angle ψ.

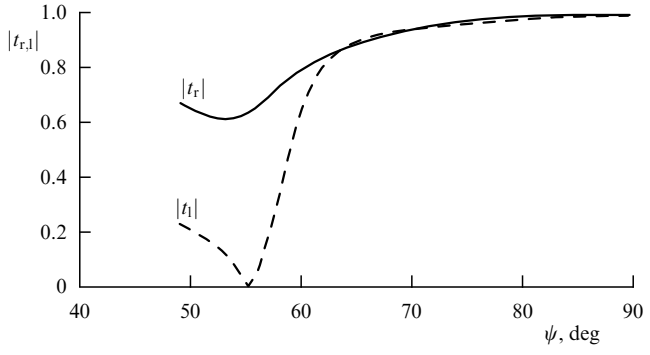

Figure 9. Dependence of the absolute values of the transmission coefficients on ψ for the right- ($|t_r|$) and left-hand ($|t_l|$) circularly polarized waves.

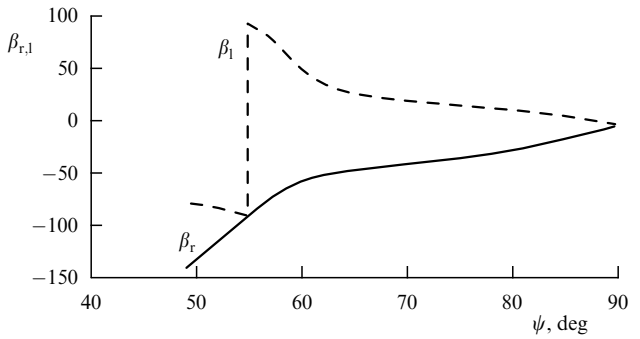

Figure 10. Dependence of phases of the transmission coefficients on ψ for the right- (β_r) and left-hand (β_l) circularly polarized waves.

3.2.3 Effect of frequency-polarization modulation. The array with parameters $\psi = 15°$ and $q = 0.34$ at $s = 0.23$ transforms circularly polarized waves into linearly polarized waves [32–34]. On the excitation with right-hand circularly polarized waves the transmitted electric field vector is directed along the cylinder axes, while the reflected field is directed perpendicular to them. On the excitation with left-hand circularly polarized waves the electric field vector of the transmitted wave is directed perpendicular to the cylinder axes, while the reflected field is directed along them. For the array involved the transmitted and reflected fields remain all but linearly polarized (the coefficient of ellipticity is less than 0.05) over a fairly wide frequency range. In the case of the right-hand circularly polarized exciting waves, the transmitted and reflected electric field vectors rotate a large angle in opposite directions at small frequency variations near the resonance. Figure 11 illustrates this effect. On excitation with the left-hand circularly polarized wave the electric field vectors virtually do not change direction. The transmitted and reflected intensities for both the polarizations weakly change and are equal approximately to 0.5 for the range of s presented in Fig. 11.

3.2.4 Effect of transmitted electric field vector turned through 90°. An array excited by linearly polarized waves was studied in Ref. [35], the angles θ between the electric field vector and

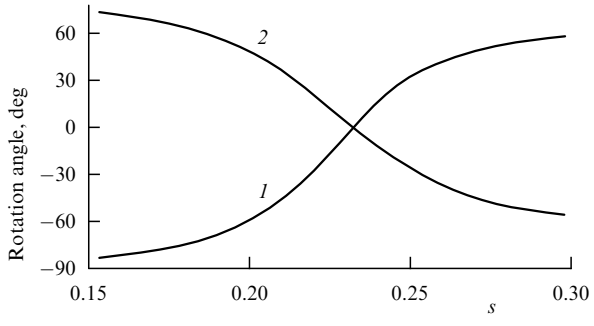

Figure 11. Frequency dependence of rotation angles for the transmitted (curve *1*) and reflected (curve *2*) electric field vectors.

the y axis were $\pm 45°$. A class of arrays was found for which the transmitted and reflected fields are linearly polarized with the electric field vector for the transmitted wave turned through 90°, while the reflected electric field vector retains the orientation of the incident field. Notice that at $\psi = 51°$ and $\psi = 63°$ complete transmission occurs for the case when $\theta = -45°$. For the orthogonal polarization ($\theta = 45°$) and certain values of ψ complete reflection sets in.

3.3 Chirotropic and filtering properties of the two-array cascade

Compared to above-considered isolated arrays, the array cascades have some new physical properties. We discuss here two properties of the cascade of two arrays involving hollow cylinders with helical electric conductivity. They are the possibility of ideal filtering of circularly polarized waves and the possibility of rotation of the electric field vector through any given angle without the power loss in the reflection at any direction of the electric field vector in the incident wave (in contrast to the effect described in Section 3.2.4).

3.3.1 Ideal filtration of circularly polarized waves. The cascade includes two identical arrays separated a distance d in parallel planes. The cylinders in both arrays have the same orientation. It is assumed that $d > p$, the latter eliminates the interaction between the arrays at nonpropagated harmonics. As is seen from Figs 8 and 9, the array with parameters $\psi = 55°$, $q = 0.87$, and $s = 0.38$ completely reflects the left-hand circularly polarized wave and partially transmits the right-hand circularly polarized wave. Since the phase of the reflection coefficient for the right-hand wave is zero, the two identical arrays spaced at $d = n\lambda/2$ $(n = 1, 2, 3)$ form a transmitting resonator, which is completely transparent for the right-hand circularly polarized wave, but completely reflects the left-hand wave.

3.3.2 Artificial chirotropic structure based on two arrays. The arrays are in parallel planes, the angle between the cylinder axes in these arrays is 2γ. The theory of the structure was developed in Ref. [36]. It was shown, among other factors, that the above chirotropic effect could be produced by fitting the parameters of the structure. Figures 12 and 13 show the frequency-dependent characteristics of the structure which turns the electric field vector through 90°. The array cascade has the following parameters: $\psi = 61.6°$, $q = 0.59$, $d = 1.9p$, and $2\gamma = 45°$. Figure 12 plots the dependence of the transmitted intensity on the normalized frequency at various orientations of the incident electric field vector. Figure 13 depicts the corresponding coefficients of ellipticity for the transmitted wave. As is seen from the figures, the structure exhibits ideal chirotropic properties at the resonance frequency $s = 0.64$, i.e. without power loss it transforms a linearly polarized wave of arbitrary direction of electric field vector into a linearly polarized wave with the electric field vector turned through 90°.

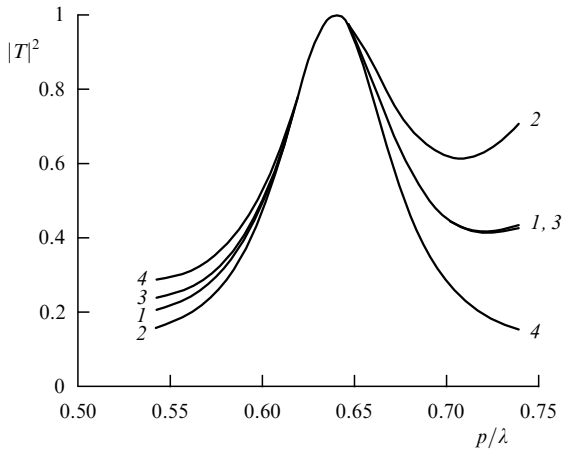

Figure 12. Frequency dependence of transmitted intensity at various orientations of the incident electric field vector: (*1*) $\vartheta = -90°$, (*2*) $\vartheta = -45°$, (*3*) $\vartheta = 0°$, (*4*) $\vartheta = 45°$.

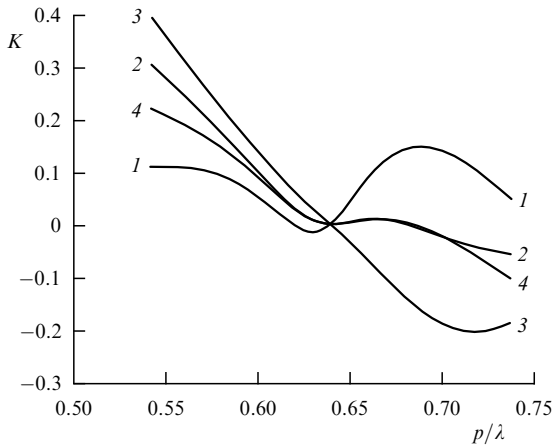

Figure 13. Frequency dependence of the coefficient of ellipticity for the transmitted wave at various orientations of the incident electric field vector: (*1*) $\vartheta = -90°$, (*2*) $\vartheta = -45°$, (*3*) $\vartheta = 0°$, (*4*) $\vartheta = 45°$.

References

1. *Advances in Complex Electromagnetic Materials* (Eds A Priou, A Sihvola, S Tretyakov, A Vinogradov) (Dordrecht, Boston, London: Kluwer Academic Publ., 1997)
2. Lindell I, Sihvola A, Tretyakov S, Viitanen A *Electromagnetic Waves in Chiral and Bi-isotropic Media* (Boston: Artech House, 1994)
3. Fedorov F I *Teoriya Girotropii* (Theory of Chirotropy) (Minsk, 1976)
4. Bohren C F *Chem. Phys. Lett.* **29** (3) 458 (1974)
5. Katsenelenbaum B Z, Sivov A N (Eds) *Elektrodinamika Antenn s Poluprozrachnymi Poverkhnostyami. Metody Konstruktivnogo Sinteza* (Electrodynamics of Antennas with Semi-transparent Surfaces. Methods of Constructive Design) (Moscow: Nauka, 1989)
6. Lindell I V, Viitanen A J *IEEE Trans. Antennas Propag.* **AP-40** (1) 91 (1992)
7. Kamenetskiy E O *IEEE Trans. Microwave Theory Tech.* **MTT-44** (3) 465 (1996)
8. Katsenelenbaum B Z *Radiotekh. Elektron.* **38** (12) 2186 (1993)
9. Tretyakov S A, Viitanen A J *Microwave and Opt. Technol. Lett.* **5** (4) 174 (1992)
10. Tretyakov S A, Viitanen A J *IEEE Trans. Microwave Theory Tech.* **MTT-43** (1) 222 (1995)
11. Landau L D, Lifshitz E M *Élektrodinamika Sploshnykh Sred* (Electrodynamics of Continuous Media) (Moscow: Nauka, 1982) [Translated into English (Oxford: Pergamon Press, 1985)]
12. Bahr A J, Clausing K R *IEEE Trans. Antennas Propag.* **AP-42** (12) 1592 (1994); Mariotte F, Tretyakov S A, Sauviac B *IEEE Antennas and Propagation Magazine* **38** (2) 22 (1996)
13. Tretyakov S A et al. *IEEE Trans. Antennas Propag.* **AP-44** (7) 1006 (1996)

14. Shevchenko V V *Radiotekh. Elektron.* **40** (12) 1777 (1995) [*J. Commun. Tech. Electron.* **40** 75 (1995)]; Kostin M V, Shevchenko V V, in *Advances in Complex Electromagnetic Materials* (Eds A Priou, A Sihvola, S Tretyakov, A Vinogradov) (Dordrecht, Boston, London: Kluwer Academic Publ., 1997)
15. Jaggard D L et al. *IEEE Trans. Antennas Propag.* **AP-37** (11) 1447 (1989)
16. Eremin Yu A, Zimnov M Kh, Katsenelenbaum B Z *Radiotekh. Elektron.* **40** (7) 1017 (1995) [*J. Commun. Tech. Electron.* **40** 132 (1995)]
17. Casey J P, Bansal R *Radio Science* **23** (6) 1141 (1988)
18. Zubov A S *Radiotekh. Elektron.* **41** (12) 1434 (1996)
19. Korshunova E N, Sivov A N, Shatrov A D *Radiotekh. Elektron.* **42** (1) 28 (1997)
20. Shatrov A D, Sivov A N, Chuprin A D *Electron. Lett.* **30** (19) 1558 (1994)
21. Vaĭnshteĭn L A *Élektromagnitnye Volny* (Electromagnetic Waves) (Moscow: Radio i Svyaz', 1988)
22. Pribyt'ko M P, Shatrov A D *Radiotekh. Elektron.* **42** (12) (1997)
23. Korshunova E N et al. *Zarubezh. Radioelektron.* (8) 44 (1997)
24. Sivov A N, Chuprin A D, Shatrov A D *Radiotekh. Elektron.* **39** (10) 1534 (1994)
25. Chuprin A D, Shatrov A D, Sivov A N, in *Proc. 24th European Microwave Conference: Cannes, 5 – 8 September, 1994*
26. Nosich A I, Shestopalov V P *Dokl. Akad. Nauk SSSR* **234** (1) 53 (1977) [*Sov. Phys. Dokl.* **22** 251 (1977)]
27. Pribyt'ko M P, Shatrov A D *Radiotekh. Elektron.* **42** (1) 23 (1997)
28. Korshunova E N, Sivov A N, Shatrov A D *Radiotekh. Elektron.* **41** (8) 911 (1996)
29. Sivov A N, Chuprin A D, Shatrov A D *Electromagnetic Waves and Electronic Systems* **1** (1) 79 (1996)
30. Chuprin A D, Shatrov A D, Sivov A N, in *Proc. Int. Conference on Chiral Bi-isotropic and Bi-anisotropic Media* held at the Pennsylvania State University on 11 – 14 October, 1995
31. Sivov A N, Chuprin A D, Shatrov A D *Radiotekh. Elektron.* **41** (5) 539 (1996)
32. Sivov A N, Chuprin A D, Shatrov A D *Radiotekh. Elektron.* **41** (8) 918 (1996)
33. Sivov A N, Chuprin A D, Shatrov A D *Pis'ma Zh. Tekh. Fiz.* **22** (1) 74 (1996) [*Tech. Phys. Lett.* **22** 37 (1996)]
34. Chuprin A D, Shatrov A D, Sivov A N, in *Proc. 11th Int. Microwave Conference MICON-96: Warsaw, 27 – 30 May, 1996*
35. Chuprin A et al., in *Proc. Int. Conference MMET-96: Lviv, 10 – 13 September, 1996*
36. Korshunova E N, Sivov A N, Shatrov A D *Radiotekh. Elektron.* **42** (11) (1997)